APPLIED ORGANOMETALLIC CHEMISTRY, VOL. 10, 579–590 (1996)

REVIEW

Electrocatalytic Reduction of Oxygen Using Water-Soluble Iron and Cobalt Phthalocyanines and Porphyrins

Nagao Kobayashi* and W. Andrew Nevin
Department of Chemistry, Tohoku University, Sendai 980-77, Japan, and Central Research Laboratories, Kaneka Corporation, 2-80, 1-Chome, Yoshida-cho, Hyogo-ku, Kobe 652, Japan

1 INTRODUCTION

There has been a great interest in the electrocatalytic reduction of oxygen using water-insoluble macromolecules. Phthalocyanines (Pcs) and also porphyrins have been applied and several review articles have been published.[1] Most of them are associated with water-insoluble catalysts and accordingly much is still unclear. For example, active forms of catalysts adsorbed on electrode surfaces and reduction mechanisms have not necessarily been well elucidated because of the difficulty of analysis of surface-adsorbed species. In order to clarify these points and the stoichiometry of oxygen reduction, we chose water-soluble Pcs and porphyrins as catalysts, because their solution chemistry is relatively well known and various spectroscopic methods can be used. Our approach has involved studying solution-phase catalysis by the electrogenerated reduced state of water-soluble metal Pcs and porphyrins, and then comparing these results with those obtained with Pcs and porphyrins that were immobilized on the surfaces of carbon electrodes. Electroreduction of oxygen using catalysts has been regarded as a model for the cathode reaction of fuel cells, but in the case of water-soluble catalysts it can also be a model for cytochrome oxidase, which reduces oxygen to water at the end of the respiratory chain.

The water-soluble porphyrins and Pcs adopted in our study are shown in Fig. 1, together with insoluble ones for comparative study. They contain either carboxyl, amino, quaternary ammonium, anilinium or pyridinium groups as peripheral substituents; in particular, compounds with pyridinium ions are soluble in water at all pH values. Of these, we first discuss the results with iron and cobalt tetrakis(1-methylpyridinium-4-yl)porphyrin (FeTMPyP[2] and CoTMPyP, respectively), since oxygen reduction was studied in most detail using these compounds.

* Author to whom all correspondence should be addressed.

2 OXYGEN REDUCTION IN THE FeTMPyP SYSTEM

2.1 Potential dependence of catalysis

The pH dependence of the $Fe^{III/II}$ redox couple of FeTMPyP was examined through the pH range 1–13 (Fig. 2). The cyclic voltammetric (CV) current–potential (i–E) curves exhibited reversible characteristics with the peak cathodic current (i_{pc}) equal in magnitude to the peak anodic current (i_{pa}) in thoroughly deoxygenated solutions. A plot of $(i_{pc}+i_{pa})/2$ as a function of pH was characterized by two regions. The first was pH 1–6, where E_{pc} remained constant at +0.15 V and independent of pH. The second was between pH 7 and 13, where E_{pc} shifted towards negative potentials with increasing pH at a rate of *ca* 60 mV/pH unit. The peak potential of the catalytic i–E wave, $E_{p,cat}$, for solutions containing equimolar concentrations of O_2 and FeTMPyP was essentially identical with that obtained for oxygen-free solutions, indicating that the potential of O_2 catalysis is related closely to the redox potential of the $Fe^{III/II}$ TMPyP couple.

2.2 Concentration dependence of catalysis

In Fig. 3A, the CV i–E curves are shown for air-saturated solutions with varying amounts of

CCC 0268–2605/96/080579–12

Received 15 May 1995
Accepted 25 May 1995

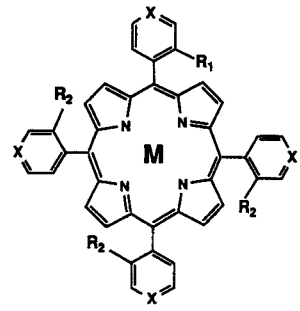

M=Fe, R_1=R_2=H, X=N^+-Me(ClO_4)$^-$: FeTMPyP
M=Co, R_1=R_2=H, X=N^+-Me(ClO_4)$^-$: CoTMPyP
M=Fe, R_1=R_2=H, X=C-$N(Me)_3^+Cl^-$: FeTMAP
M=Co, R_1=R_2=H, X=C-$N(Me)_3^+Cl^-$: CoTMAP
M=Fe, R_1=R_2=H, X=C-COOH: FeTCPP
M=Fe, R_1=R_2=H, X=C: FeTPP
M=Fe, R_1=NH_2, R_2=H, X=C: FeMOAP
M=Fe, R_1=R_2=NH_2, X=C: FeTOAP

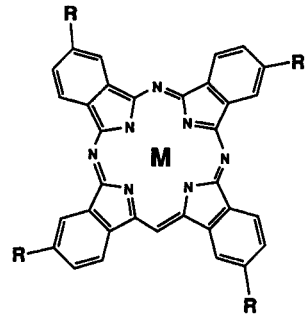

M=Fe, R=COOH: FeTCPc
M=Co, R=COOH: CoTCPc
M=Co, R=$(CH_2)_3N^+(Me)(Et)_2I^-$: CoAmPc

Figure 1 Structures and abbreviations of porphyrins and phthalocyanines treated in this study.

FeTMPyP. Curve a in this Figure represents the i–E waves for oxygen in the absence of FeTMPyP. As shown, as the iron porphyrin concentrations increased from 0.02 to 0.99 mM, $E_{p,cat}$ moved towards more positive potentials. At a catalyst/oxygen concentration ratio of 4:1, $E_{p,cat}$ is 40 mV more positive than the E_{pc} value of Fe^{III}TMPyP in oxygen-free solutions (broken line in Fig. 3A). This indicates that the kinetic rates of electron transfer (E) and chemical (C) steps are very fast. The experimentally observed shift in $E_{p,cat}$ with FeTMPyP concentration is in

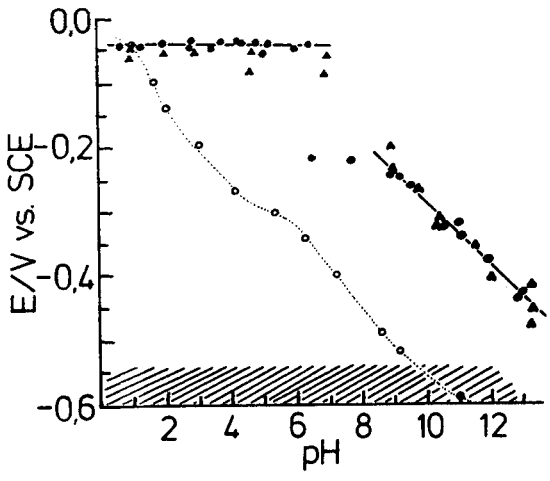

Figure 2 Potential vs pH for the various reduction processes. ●, Reduction of Fe^{III}TMPyP; ▲, reduction of O_2 in the presence of Fe^{II}TMPyP; ○, reduction of O_2 in the presence of Fe^{II}TCPP. The hatched region indicates the potentials of O_2 reduction in the absence of catalyst.

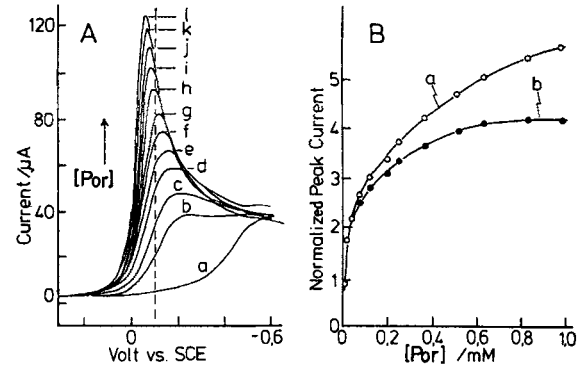

Figure 3 (A) The cathodic part of the cyclic voltammograms for the reduction of O_2 at various concentrations of FeTMPyP: $[O_2]$=0.24 mM. [FeTMPyP] (mM): curve a, 0.00; b, 0.022; c, 0.044; d, 0.085; e, 0.13; f, 0.20; g, 0.25; h, 0.37; i, 0.51; j, 0.63; k, 0.83; l, 0.99. The broken line indicates the $Fe^{III/II}$TMPyP potential under N_2. (B) Plot of the peak normalized current vs Fe^{III}TMPyP concentration. Curve a, $i_{p,N}$ vs [FeTMPyP]; curve b, $i_{p,N,cor}$ vs [Fe^{III}TMPyP]. $[O_2]$=0.24 mM; scan rate=0.05 V s^{-1}. $i_{p,N=1}$ is calculated for the one-electron reduction of O_2 using the Randles–Sevcik equation and the concentration and diffusion coefficient of O_2.

agreement with computer-simulated potential values (Section 2.4) for an EC mechanism when the rate constant of the E step is *ca* 6×10^{-3} cm s^{-1} and the rate constant of the C step is greater than *ca* 5×10^{6} M $^{-1}$ s^{-1}.

In Fig. 3B, a normalized peak function, $i_{p,N}$, is plotted against the FeTMPyP concentration for oxygen catalysis. The normalization involves the $i_{p,cat}$ value taken from Fig. 3A divided by the peak current, $i_{p,N=1}$, that would result if oxygen were reduced by a one-electron process to the superoxide ion. The $i_{p,N=1}$ value was calculated from the Randles–Sevcik equation,[3] which is valid for a reversible, diffusion-controlled electrode reaction. As can be seen from this Figure, $i_{p,N}$ increases rapidly with the FeTMPyP concentration of *ca* 5×10^{-4} M. Curve b of this Figure is the corrected normalized current, $i_{p,N,cor}$, which is calculated by subtracting from $i_{p,cat}$ the peak current contributed by the reduction of Fe^{III}TMPyP to Fe^{II}TMPyP, as determined from the reduction of the iron porphyrin in oxygen-free solutions. The $i_{p,cat,cor}$ plot yields a limiting value of 4.1, suggesting that oxygen is being reduced to water when the FeTMPyP/oxygen concentration ratio becomes greater than *ca* 2:1. The $i_{p,cat}$ value depends on the extent of overlap between the wave for O_2 catalysis and that of the mediator. Computer simulation of the EC mechanism (Section 2.4) indicates that the $i_{p,cat}$ value maximizes when the concentrations are such that the catalytic wave coincides with and is 'stacked' onto the mediator/catalyst wave. Thus, data in Fig. 3 clearly show that oxygen can be reduced catalytically by the iron porphyrin and that the extent of the reduction depends on the concentration ratios of porphyrin to oxygen.

The stoichiometry of O_2 catalysis by FeTMPyP was also evaluated by conducting CV experiments in a thin-layer cell (coulometry). Under the four-electron reduction condition in Fig. 3B, on the initial cathodic scan the charge corresponded to a four-electron reduction of O_2 and a one-electron reduction of Fe^{III}TMPyP. During all subsequent scans, the cathodic and anodic charges were equal and accounted for by the $Fe^{III/II}$TMPyP redox process.

2.3 Hydrogen peroxide reduction by Fe^{II}TMPyP

Although not shown, detailed analysis of *i–E* waves for O_2 reduction showed that, at low scan rates and the higher iron porphyrin/oxygen concentration ratios, $i_{p,N,cor}$ was *ca* 4, whereas at high scan rates and lower concentration ratios, the calculated value approached 2, suggesting that the mechanism of O_2 reduction by iron porphyrin involves a series pathway with hydrogen peroxide (H_2O_2) as a possible initial product. Thus H_2O_2 reduction experiments have been conducted at pH 1 after demonstration that the rates of H_2O_2 dismutation by Fe^{III}TMPyP and decomposition of Fe^{III}TMPyP by H_2O_2 were slow at this pH. Plots of $i_{p,cat}$ vs $\nu^{1/2}$ of CV *i–E* waves were linear over a wide range of scan rates and their slope gave a stoichiometric ratio value of 2.1, which is indicative of a two-electron reduction of H_2O_2. Thin-layer cell coulometry also gave an *n* value of 1.9, indicating that H_2O_2 is quantitatively reduced to water. Also, as in the reduction of O_2, the potential for H_2O_2 catalysis is governed by the $Fe^{III/II}$TMPyP redox couple, again consistently with an EC mechanism.

2.4 Computer simulations

CV *i–E* profiles for O_2 catalysis by iron porphyrin were simulated by the use of computer programs which were designed to account for the kinetic rates of both the heterogeneous electron-transfer rate, k_s, of reaction [1] below and the homogeneous reactions, k_f, the differences in the diffusion coefficients of the reactants, the concentrations of the electroactive and other species in the reaction sequence, and the stoichiometry (*N*) of any homogeneous reactions.[4] The different EC catalytic mechanisms for oxidation catalysed by Fe^{II}TMPyP were considered (Eqns [1]–[4]).

(I) E step:

$$Fe^{III}TMPyP + e^- \xrightarrow{k_s} Fe^{II}TMPyP \qquad [1]$$

and C steps:

$$2Fe^{II}TMPyP + O_2 + 2H^+ \xrightarrow{k_{f1}} 2Fe^{III}TMPyP + H_2O_2 \qquad [2]$$

(II) Reaction [1] followed by:

$$4Fe^{II}TMPyP + O_2 + 4H^+ \xrightarrow{k_{f1}} 4Fe^{III}TMPyP + 2H_2O \qquad [3]$$

(III) Reactions [1] and [2] followed by:

$$2Fe^{II}TMPyP + H_2O_2 + 2H^+ \xrightarrow{k_{f2}} 2Fe^{III}TMPyP + 2H_2O \quad [4]$$

where reactions [2]–[4] reflected the reactant stoichiometry in the homogeneous steps. The *i*–*E* profiles simulated for mechanisms I and II above could not account for the experimental results over a wide variation of scan rates and iron porphyrin/oxygen concentration ratios. The best fit between experimental and simulated *i*–*E* profiles was obtained consistently with the modelling of mechanism III (Fig. 4). Thus, the results of computer simulation also suggested that O_2 reduction proceeds via H_2O_2 as an intermediate.

2.5 An active form of catalyst

In order to obtain an insight into the active forms of catalyst, magnetic circular dichroism (MCD) measurements were performed (Fig. 5). MCD is sensitive to both the spin and oxidation states of metal complexes and therefore has been applied particularly to phthalocyanines and porphyrins. Together with the results of electrochemical speciation,[5] the characteristic Soret band MCD curve (large plus and small minus sign seen from the longer wavelength) indicates that the active form is a pentacoordinated divalent high-spin iron complex.[6] Scheme 1 shows the relationship of the various FeTMPyP species in aqueous solution.

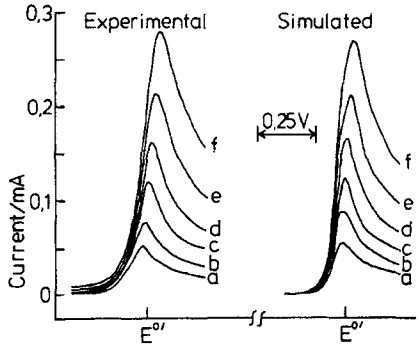

Figure 4 Experimental and simulated cyclic voltammetric curves for the reduction of O_2 by $Fe^{II}TMPyP$ ($[O_2] = 0.24$ mM; $[Fe^{III}TMPyP] = 0.53$ mM) at the following scan rates (in V s^{-1}): (a) 0.010; (b) 0.025; (c) 0.050; (d) 0.100; (e) 0.200; (f) 0.400.

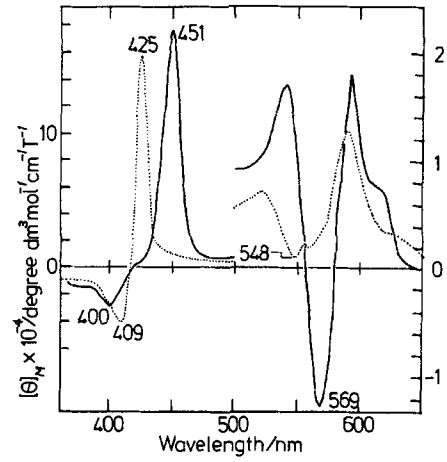

Figure 5 Magnetic circular dichroism of $Fe^{II}TMPyP$ generated in an optically transparent thin-layer electrode (OTTLE) cell (solid lines) in pH 4.7 acetate buffer, and that of $Fe^{II}TCPP$ (dotted lines) in pH 9.1 Briton–Robinson buffer.

3 OXYGEN REDUCTION IN THE CoTMPyP SYSTEM

3.1 Homogeneous case

When dissolved in aqueous solution, cobalt in CoTMPyP is in the trivalent diamagnetic low-spin state, in contrast to iron in FeTMPyP which is in the trivalent paramagnetic high-spin state.[7] The CVs of $Co^{III}TMPyP$ (0.05 M H_2SO_4) in the absence and presence of oxygen are compared in Fig. 6A, traces a and b.[8] The peak current in the presence of oxygen indicates that O_2 is quantitatively reduced to H_2O_2 by a two-electron process. The close correspondence between the potential for catalysis and the redox potential of the $Co^{III/II}TMPyP$ couple suggests an EC-type

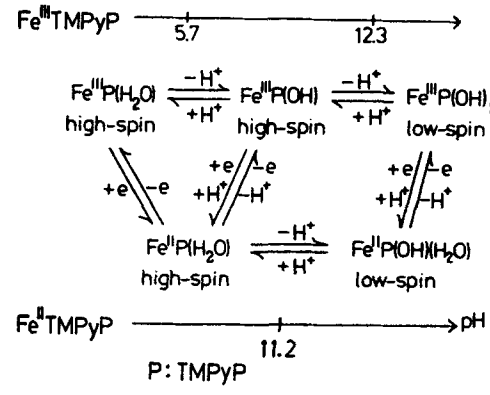

Scheme 1

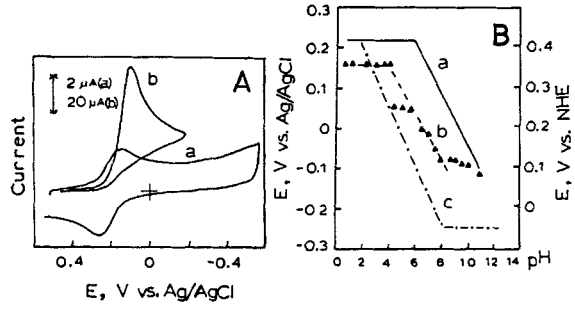

Figure 6 (A) Cyclic voltammograms of 2.69×10^{-4} M CoTMPyP in 0.05 M H_2SO_4 (a) in N_2- and (b) in O_2-saturated solution. Electrode area = 0.144 cm^2; scan rate = 20 mV s^{-1}. (B) Various potentials plotted vs pH: (a) formal potential, $E^{0\prime}$, vs pH for $Co^{III/II}$TMPyP solution without oxygen; (b) $E_{p,cat}$ vs pH for 2.7×10^{-4} M CoTMPyP in air-saturated solutions (solid triangles are data points); (c) E_p and $E_{p,cat}$ for adsorbed CoTMPyP in the absence and presence of oxygen, respectively.

mechanism similar to that discussed above for FeTMPyP. However, in the present case, if the $E_{p,cat}$ vs pH is plotted as in curve b of Fig. 6B, the $E_{p,cat}$ values are seen to be shifted to slightly negative of the reversible $E^{0\prime}$ values of the $Co^{III/II}$TMPyP couple in the pH 1–4 range. This shift results from plotting the peak of the catalytic wave rather than a value of the potential near the foot of the catalytic wave, where Co^{II}TMPyP begins to be generated, and the overpotential for reducing Co^{III}TMPyP. However, as the pH becomes more alkaline, a double wave appears for the catalysis until, at pH 4, only the catalytic wave at the more negative potential is seen (see CV wave vs pH in Fig. 7A). Such a shift in $E_{p,cat}$ is not explained by an acid–base equilibrium of the solution Co^{III}TMPyP since its

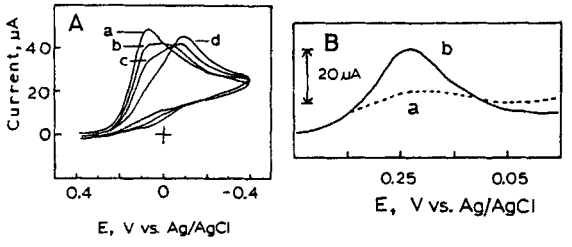

Figure 7 (A) Cyclic voltammograms of catalytic O_2 reduction by 2.69×10^{-4} M CoTMPyP at pH 3–4 (electrode area = 0.144 cm^2; scan rate = 20 mV s^{-1}): (a) pH 3.0; (b) pH 3.3; (c) pH 3.6; (d) pH 4.0. (B) Differential pulse voltammograms of surface-adsorbed CoTMPyP in 0.05 M H_2SO_4 solution (electrode area = 0.144 cm^2; scan rate = 5 mV s^{-1}): (a) N_2-saturated; (b) O_2-saturated.

pK_a values are 6 and 10.[7] In the pH 6–8 range, $E_{p,cat}$ decreases at a rate of 60 mV/pH unit and then becomes nearly independent of pH at pH > 8. At pH > 9, anodic wave is observed due to the oxidation of H_2O_2 (confirmed by the enhancement of the anodic peak current when H_2O_2 was added). In contrast to FeTMPyP, Co^{II}TMPyP reacts much more slowly with H_2O_2.

3.2 Adsorbed case

Since the above pH dependence of the $Co^{III/II}$TMPyP couple and O_2 catalysis is peculiar and different from that in the FeTMPyP system, O_2 catalysis by adsorbed CoTMPyP was examined in order to clarify the behavior appearing in Fig. 6. If a glassy carbon electrode is exposed to a Co^{III}TMPyP solution, removed, washed with distilled water, and then immersed in an air-saturated 0.05 M H_2SO_4 solution without cobalt porphyrin present, a well-defined O_2 catalytic wave can be observed with the $E_{p,cat}$ occurring near the redox potential of the solution Co^{III}TMPyP. The presence of adsorbed cobalt porphyrin is evident in the differential pulse voltammograms, as shown in Fig. 7B, for background (trace a) and for the electrode with adsorbed porphyrin (trace b) in the presence of oxygen. At pH 1–10, there is a close correspondence between the differential pulse voltammetric E_p values and the adsorbed porphyrin and the CV $E_{p,cat}$ values. However, surprisingly, the pH dependence of the adsorbed case is considerably different from the solution case as shown by trace c in Fig. 6B. Thus, the difference in the pH dependence of the redox potential between the solution and the adsorbed CoTMPyP suggests that, as the pH is increased, the catalysis of O_2 reduction by adsorbed CoTMPyP becomes less important when Co^{III}TMPyP is present in solution. This gradual transition from a composition solution and an adsorbed CoTMPyP to predominantly a CoTMPyP catalysis solution explains the CV's behaviour as seen in Fig. 7A. A discontinuity at pH 4 is believed to arise from the fact that the formal potential of the solution $Co^{III/II}$TMPyP becomes more positive than that of the O_2/H_2O_2 redox couple. On the other hand, the thermodynamics become unfavourable for the solution of cobaltous porphyrin to reduce O_2 to H_2O_2 at pH > 4. Thus O_2 is not catalysed until the electrode potential moves to more negative values where the adsorbed Co^{III}TMPyP is

reduced. Even at adsorbed CoTMPyP, H_2O_2 is produced quantitatively.

4 OXYGEN REDUCTION IN OTHER WATER-SOLUBLE PORPHYRIN SYSTEMS

4.1 Tetrakis(*N,N',N''*-trimethylanilinium)porphyrin systems

Iron[9] and cobalt[10] derivatives of this porphyrin (abbreviated as Fe and CoTMAP, respectively) have catalytic activity for O_2 reduction. These porphyrins are water-soluble but apt to be adsorbed strongly on electrode surfaces. At pH values of less than 2, the $Fe^{III/II}$ redox couple of dissolved FeTMAP is observed at -0.275 V vs SCE, but simultaneously that of adsorbed FeTMAP appears at *ca* -0.1 V. When oxygen is admitted, it is reduced at the latter potential, indicating that O_2 reduction is determined essentially by a surface redox couple in an EC catalysis mechanism. Rotating ring disc electrode (RRDE) experiments showed that the reduction proceeds through a four-electron process to yield water as the major product.

In the case of the CoTMAP system, the reduction potential of both dissolved and adsorbed Co^{III}TMAP and oxygen coincide over the pH range from 1 to 12, indicating that O_2 is reduced by an EC mechanism. The most characteristic aspect of this porphyrin is, however, that *O_2 is reduced to water through a four-electron reduction in acidic solution* (in general in the presence of cobalt complexes, O_2 is reduced to hydrogen peroxide only). The reduction takes place at *ca* 0.07 V vs SCE at pH 1.

4.2 Porphyrins containing either carboxyl or amino group(s)

O_2 reduction by tetracarboxyphenylporphyrin iron complex, FeTCPP, has also been explained by an EC mechanism.[11] As for FeTMPyP, when the [FeTCPP] was small, H_2O_2 was produced as the major product, but at higher [FeTCPP] water was produced via H_2O_2, and the active form of the catalyst was a pentacoordinated divalent iron high-spin species (see the dotted MCD lines in Fig. 5). The pH dependence of catalysis alone is different from that in the FeTMPyP system, showing *ca* 55 mV/pH unit dependence (Fig. 2). This suggests that a proton is associated in both E and C steps. As for other porphyrin systems, O_2 reduction at surface-immobilized FeTCPP occurs at more anodic potentials than in the dissolved FeTCPP system.[12]

Tetraphenylporphyrins containing four amino groups show high catalytic activity towards O_2 reduction, particularly in terms of the amount required for a four-electron reduction (in the porphyrin dissolved system, approximately two orders of magnitude smaller than FeTCPP).[2h, 13, 14] That the immobilized amino group is also effective is shown in the results of Figs 8 and 9. Figure 8 compares the RRDE response in the O_2 reduction at electrodes immobilized with iron porphyrins containing four, one and zero amino groups, i.e. FeTOAP, FeMOAP, and FeTPP. In each set of curves, the

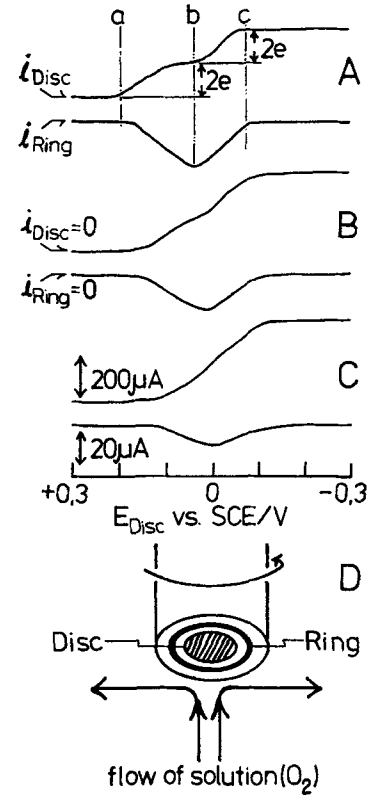

Figure 8 *i–E* curves during the reduction of O_2 at a rotating glassy carbon (GC)–platinum ring electrode in pure O_2-saturated 0.05 M H_2SO_4. The GC disc (0.22 cm^2) was coated with 2×10^{-9} mol cm^{-2} of (A) FeTPP, (B) FeMOAP and (C) FeTOAP. Ring electrode potential = 1.2 V vs SCE; rotation rate = 100 rpm. (D) Structure of RRDE.

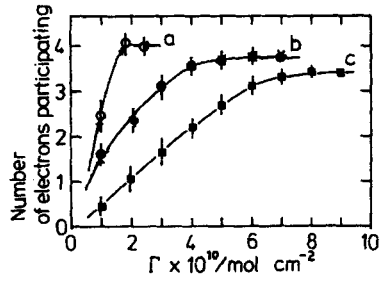

Figure 9 Relationship between O_2 reduction peak current and surface coverage of iron porphyrins on a GC electrode as obtained by the GC method. (a) FeTOAP, (b) FeMOAP and (C) FeTPP. Bars indicate the limit of error. The abscissa (surface coverage) was obtained from the value of [iron porphyrin]/(area of adsorption).

upper one represents the response at a disc, i.e. the O_2 reduction current, while the lower one is the response at a ring whose potential is set so that H_2O_2 can be oxidized (+1.0–1.2 V vs SCE). That is, when the disc potential is scanned from the positive to the negative direction, if H_2O_2 is produced as an intermediate it is detected at the ring electrode. In all cases H_2O_2 was detected and its amount reached a maximum at *ca* 0 V vs SCE. But in the case of a tetraphenylporphyrin without the amino group (FeTPP), this amount is larger than for the case of tetra(*o*-aminophenyl)porphyrin (FeTOAP) and conversely the limiting disc currents are larger for the latter porphyrin (when normalized, $n=3.5$ and 4.1 for FeTPP and FeTOAP, respectively). Also, as shown in Fig. 9, which shows the relationship between the O_2 reduction peak current (in the CV method) and surface coverage of iron porphyrins on glassy carbon electrodes, the amount of porphyrin required to attain saturation of the current differs from porphyrin to porphyrin, decreasing markedly in the order FeTPP>FeMOAP>FeTOAP. Although complexes with amino groups are known to enhance the non-electrochemical H_2O_2 decomposition process,[15] the real role of the amino group is unclear at present. However, since amino groups are classed as electron-donating groups, back-donation of electrons may increase the electron density at iron, thereby facilitating electron transfer from iron to oxygen.[16]

5 OXYGEN REDUCTION IN SYSTEMS CONTAINING DISSOLVED IRON OR COBALT TETRACARBOXYPHTHALOCYANINE[17]

The concentration dependence of O_2 catalysis by iron and cobalt tetracarboxyphthalocyanine (abbreviated as FeTCPc and CoTCPc, respectively) was examined at a fixed scan rate (Fig. 10A, B). As for FeTMPyP (Fig. 3A), as the [FeTCPc] increased, a main O_2 reduction peak potential moved towards positive potentials with a concomitant increase in its current, and at [FeTCPc] $\simeq 3\times10^{-5}$ M the change stopped, while the prewave at *ca* −0.2 V kept increasing with an increase in [FeTCPc]. For the CoTCPc

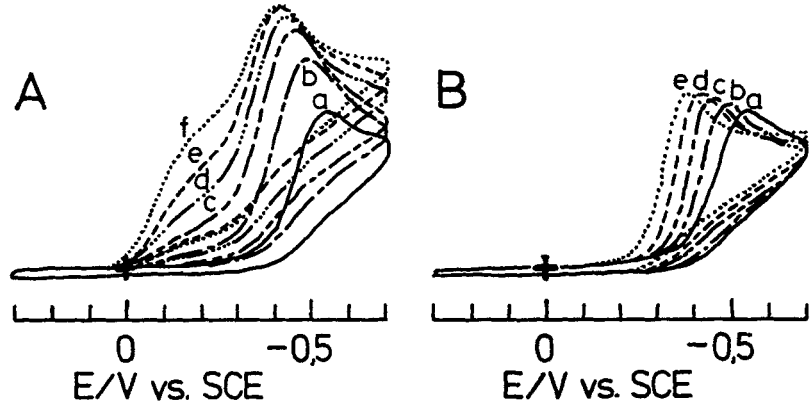

Figure 10 (A) Cyclic voltammograms for the reduction of O_2 (air-saturated, *ca* 0.24 mM) in 0.1 M bicarbonate solution (pH 9) containing various concentrations of FeTCPc (in M): (a) 0.0; (b) 1.43×10^{-7}; (c) 2.28×10^{-6}; (d) 1.14×10^{-5}; (e) 3.42×10^{-5}; (f) 1.14×10^{-4}. (B) Same as (A) but in the presence of various concentrations of CoTCPc (in M): (a) 0.0; (b) 1.44×10^{-7}; (c) 2.30×10^{-6}; (d) 3.44×10^{-5}; (e) 1.38×10^{-4}. Scan rate=0.08 V s^{-1}.

catalyst also, an anodic shift of the O_2 reduction was observed with an increase in its concentration. However, the accompanying increase in peak current was not so obvious (as for FeTCPc, saturated at *ca* 3×10^{-5} M). So long as the concentrations of the catalysts were fixed, there was no potential dependence of the catalysis at pH values from 7.8 to 13, precluding participation of protons or hydroxyl anions.

Oxygen reduction was examined also by the RRDE method. In Fig. 11A curves a, b, and c respectively show the *i–E* responses for O_2 reduction in pure O_2-saturated solution in the presence of FeTCPc and CoTCPc, and in their absence. Although the homogeneously dissolved catalysts and oxygen are brought to the surface of the RRDE, a calculation based upon the theory of RRDE indicated that the contribution of the catalysts to the observed current is only a few per cent. In the presence of FeTCPc, O_2 reduction commenced at *ca* 0 V and when the disc electrode potential (E_{disc}) reached *ca* −0.45 V, the amount of the current matched approximately that expected from the Levich equation[18] for a four-electron reduction of oxygen. On the other hand, as curve b shows, O_2 reduction in the presence of CoTCPc proceeded in two steps. The

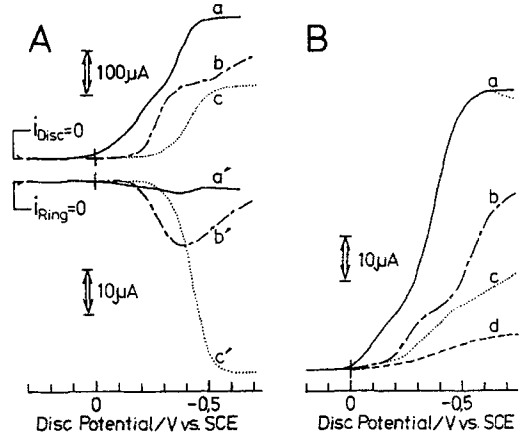

Figure 11 (A) Ring-disc *i–E* curves for the reduction of O_2 in the presence of 1.14×10^{-4} M FeTCPc (curves a and a') or 1.20×10^{-4} M CoTCPc (curves b and b') and in the absence of catalysts (curves c and c'). The solution was pure O_2-saturated, 0.1 M bicarbonate solution (pH 9.0), and the ring potential was set at +1.2 V. (B) *i–E* curves for the reduction of 0.8 mM H_2O_2 at a rotating GC disc (a) in the presence of 1.14×10^{-4} M FeTCPc, (b) in the presence of 1.20×10^{-4} M CoTCPc, and (c) in the absence of catalyst. Curve d is an *i–E* curve for N_2-saturated, 0.1 M bicarbonate solution (pH 9.0) in the absence of H_2O_2.

cathodic current began to increase at $E_{disc}=ca$ −0.2 V but its rate of increase fell off in the region of $-0.4<E_{disc}<-0.5$ V and again increased at more negative potentials. Corresponding to these *i–E* curves a, b and c at discs, the responses at rings (curves a', b' and c', respectively) were obtained (Fig. 11A). Although the anodic current was detected in all cases, the amount was different, decreasing markedly in the sequence c'>b'>a'. In the case of CoTCPc, the ring current increased but, after reaching a maximum, it decreased. By comparing curves b and b', the first stage is rationalized to be an O_2 to H_2O_2 process and the second step a partial reduction of H_2O_2 to H_2O. The disc current at the potential where the ring current reached a maximum corresponds to the current from a two-electron reduction of oxygen. Thus, it is suggested that the O_2-to-H_2O_2 process occurs at a more positive potential than that from H_2O_2 to H_2O. As curve a' shows, O_2 reduction in the presence of FeTCPc also appears to proceed via H_2O_2.

Reduction of H_2O_2 was examined in oxygen-free solutions (Fig. 11B). In both FeTCPc and CoTCPc systems, H_2O_2 was reduced in the potential range where O_2 was reduced, although in the latter system more current was observed at potentials more negative than −0.5 V, as anticipated from Fig. 11A.

In order to obtain the number of electrons involved in the reduction, the Levich equation[18] was used. The values were 3.78 and 2.08 for systems containing FeTCPc and CoTCPc, respectively. Since the intercept of Koutecky–Levich plots[18] (not shown) at an infinitely high rotation rate was zero, the rates of reaction proved to be too fast to measure with the RRDE ($>10^7$ M^{-1} s^{-1}). FeTCPc trapped in poly-β-cyclodextrin also catalyses a four-electron reduction of O_2 at alkaline pH, but a two-electron reduction at acidic pH.[19]

In order to obtain information on the oxidation and spin state of the central metals of active forms of the catalysts, electronic absorption and MCD spectra were recorded. Although the oxidation state of iron in iron phthalocyanines is generally 2+, FeTCPc in pH 9 solution has been shown to exist as a mixture of at least the iron(III) high- and low-spin complexes because of the electron-withdrawing carboxyl groups.[20] The spectrum in Fig. 12A (dotted line) represents this state. However, when the potential of the working electrode in the optically transparent

thin-layer electrode (OTTLE) cell was brought to *ca* −0.45 V, a well-defined spectrum drawn as a solid line was obtained (the spectrum changed dramatically at *ca* −0.4–0.45 V, where catalytic O_2 reduction occurs). From the presence of a diagnostic absorption peak at 440 nm which can be assigned to a charge-transfer transition from iron to the axial ligand,[21] the species was judged to be in the low-spin iron(II) state.

In the absence of applied potential, cobalt in CoPcs is generally divalent. The curve shown by the dotted line in Fig. 12B represents the spectrum of Co^{II}TCPc, aggregated to some extent in a cofacial manner.[22] However, when the potential of OTTLE was changed to *ca* −0.4 V, a drastic spectral change was always observed between −0.3 and −0.4 V and the spectrum shown by the solid line was obtained. From the appearance of the characteristic new peak at 467 nm which can be assigned to charge transfer from cobalt to ligand,[23] and the corresponding negative Faraday *A*-term in MCD spectrum (not shown),[23a] the active species was found to be a low-spin cobalt(I) complex.

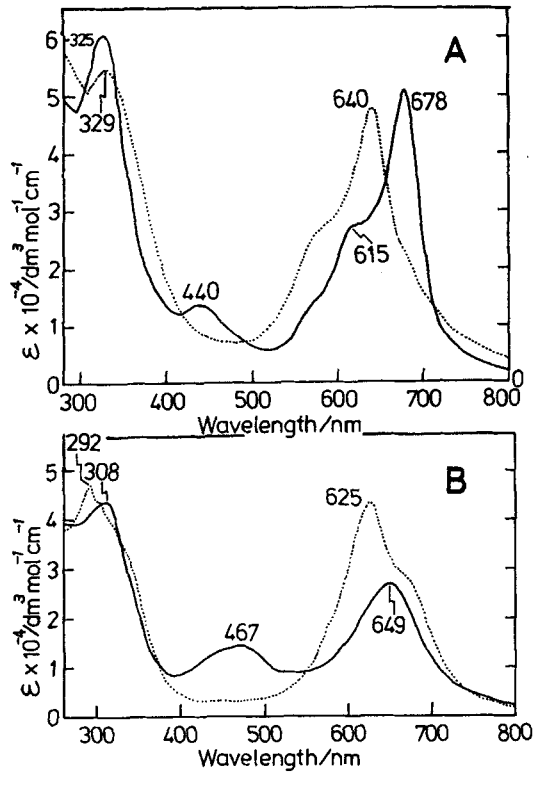

Figure 12 The electronic absorption spectra of (A) Fe^{III}TCPc and (B) Co^{II}TCPc in the absence of the applied potential (dotted lines); and electrochemically generated Fe^{II}TCPc and Co^{I}TCPc species (solid lines). Applied potential = −0.45 and −0.42 V vs SCE for Fe^{II}TCPc and Co^{I}TCPc, respectively.

From the results mentioned above, the O_2 electroreduction in the presence of FeTCPc and CoTCPc dissolved in solution could be judged to proceed by an EC catalytic regeneration mechanism, although there may be a slight potential difference between the O_2-to-H_2O_2 and the H_2O_2-to-H_2O process. However, in contrast to the Fe-TMPyP, CoTMPyP and FeTCPP systems, O_2 reduction potential does not depend on the pH values of solution, and the reduction of the overpotential by the catalysts is smaller than in porphyrin systems.

6 OXYGEN REDUCTION IN THE TETRAKIS[3-(DIETHYL-METHYLAMMONIO)PROPYL] PHTHALOCYANINATOCOBALT SYSTEM[24]

The CoPc in this section (abbreviated as CoAmPc) is the first amphiphilic Pc and therefore soluble in many solvents such as water, alcohols, acetonitrile, chloroform, benzene, dioxane and *N*,*N*-dmethylformamide (DMF), which gives us the rare opportunity to connect and compare its chemistry in organic solvents and in water. For example, it was found that it exists as dimers in water and as monomers in some organic solvents, including acetonitrile, dioxane, chloroform, propanol and DMF. Accordingly, CoAmPc was first adsorbed on to glassy carbon electrodes in acetonitrile and aqueous solution, and their catalytic activities were compared. As seen in Fig. 13, an interesting phenomenon was observed—namely, that both $Co^{II/I}$AmPc and O_2 reduction potentials at electrodes prepared in acetonitrile (curves a and c) lie at more anodic potentials than those prepared in aqueous solution (curves a′ and c′), although the relatively symmetrical $Co^{II/I}$AmPc redox patterns under nitrogen suggest the absence of significant interaction among the adsorbed species (this implies that, although CoAmPc exists as a dimer in water, the dimer structure may not be retained when it is immobilized on glassy carbon by adsorption). As curves c and c′ show, oxygen is reduced catalytically to hydrogen peroxide at a much more positive potential than the $Co^{II/I}$

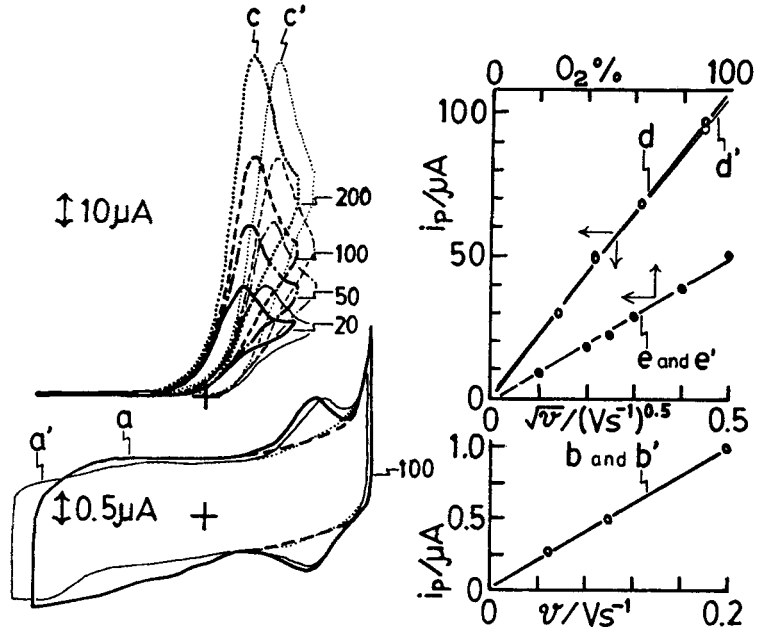

Figure 13 Cyclic voltammograms at CoAmPc-adsorbed GC electrodes (area 0.070 cm^2) in water at pH 7.0. Adsorption was carried out either in 10^{-4} M acetonitrile solutions (bolder curves and lines, denoted by a–e), or in 10^{-4} M aqueous solutions (finer curves and lines denoted by a′–e′) for 10 min. Numbers on curves indicate scan rate in mV s^{-1}. Curves a and a′, responses in deaerated solution; curves c and c′, in O_2-saturated solution. Line b and b′ indicates the relationship between peak currents in curve a or a′ (*ca* −0.31 or *ca* −0.33 V) and scan rate. Lines d and d′ show the relationship between peak currents in curves c or c′ and the square root of scan rate, and line e and e′ demonstrates the catalytic O_2 reduction peak current vs O_2 concentration relationship obtained at a sweep rate of 50 mV s^{-1}.

redox couple in curves a and a′, but there is no difference in the peak height between the two types of modified electrode over a wide-sweep range.

Potentials for the $Co^{II/I}$ couple and O_2 reduction peak at pH 1 and 7 are summarized in Table 1. The $Co^{II/I}$ redox potentials at pH 1 lie at much more anodic potentials than at pH 7, but the O_2 reduction potentials at pH 1 do not shift greatly from those at pH 7 and are equal to $Co^{II/I}$ redox potentials at pH 1. Thus, the O_2 reduction in the catalyst-adsorbed system at pH 1 can be explained by an EC catalyst regeneration mechanism, but that at pH 7 may be different, since the potential difference between the $Co^{II/I}$ redox couple and O_2 reduction is very large (*ca* 200 mV). A reaction mechanism such as a CE (chemical step followed by electron transfer)

Table 1 Potentials (V) at CoAmPc-modified electrodes and bare glassy carbon electrodes

	Electrode with adsorbed CoAmPc					
	From 10^{-4} M acetonitrile solution		From 10^{-4} M aqueous solution		Dissolved CoAmPc system	
	pH 1	pH 7	pH 1	pH 7	pH 1	pH 7
$Co^{II/I}$ (V)[a]	−0.12	−0.31	−0.15	−0.33	−0.43	−0.38
O_2 redn (V)	−0.12	−0.12	−0.15	−0.17	−0.17	−0.22

[a] Defined as (cathodic peak potential+anodic peak potential)/2.

mechanism (Eqns [5] and [6]) may be considered.

$$Co^{II}AmPc + O_2 \rightarrow Co^{II}AmPc{-}O_2 \quad [5]$$

$$Co^{II}AmPc{-}O_2 + 2e^- + 2H^+ \rightarrow Co^{II}AmPc + H_2O_2 \quad [6]$$

Judged from the amount of current, the final product was H_2O_2. Judging from the large potential difference between the $Co^{II/I}$ couple and O_2 catalysis, responses in the dissolved-CoAmPc system may also be rationalized by the CE mechanism.

7 CONCLUDING REMARKS

The results of electroreduction of oxygen in the presence of water-soluble porphyrins and phthalocyanines may be summarized as follows.

(1) In the catalyst-dissolved system, iron and cobalt complexes generally catalyse four- and two-electron processes to H_2O and H_2O_2, respectively, and the reduction is explained, in most cases, by an EC catalyst regeneration mechanism.

(2) In the presence of iron cattalysts the reduction often proceeds via H_2O_2, while in the case of cobalt catalysts a four-electron reduction to water is quite seldom known, and then only in highly acidic solution.

(3) If catalysts are adsorbed on to the electrode surface, their metal redox couples often shift to more anodic potentials than in solution, and oxygen is reduced at these or more positive potentials. In the former case, the reaction can be explained by a surface-adsorbed EC mechanism, while in the latter case it is often rationalized by a CE mechanism.

(4) In order to reduce the overpotential of O_2 reduction, porphyrin catalysts are generally better than phthalocyanine catalysts, and acidic solution is more favourable than alkaline solution.

(5) In the cases of iron porphyrins so far examined active forms of catalysts are all pentacoordinated, divalent, high-spin species, while in the cases of phthalocyanines these are divalent iron, low-spin and monovalent cobalt, low-spin species.

(6) Functional groups at the periphery of macrocycles do affect the catalysis. Electron-donating groups heighten the activity.

(7) When catalyst-adsorbed electrodes are used, those prepared in organic solution may reduce oxygen at more anodic potentials than those prepared in aqueous solution.

Although not mentioned in the body of this review, homogeneously dissolved $Mn^{II}TMPyP$ also catalyses the O_2-to H_2O_2 process at [MnTMPyP] values more than *ca* 5×10^{-5} M by an EC catalytic regeneration mechanism. Its active species is in a high-spin divalent state.[25]

REFERENCES

1. (a) H. Jahnke, M. Schonborn and G. Zimmermann, *Topics Curr. Chem.* **61**, 133 (1976); (b) M. R. Tarasevish and K. A. Radyushikina, *Russ. Chem. Rev. Engl. Transl.* **49**, 1498 (1980); (c) F. van den Brink, E. Barendrecht and W. Vissher, *Recl. Trav. Chim. Pays-Bas* **99**, 523 (1980); (d) J. A. R. van Veen and J. F. van Baar, *Rev. Inorg. Chem.* **4**, 293 (1982); (e) D. J. Shiffrin, *Electrochemistry* **8**, 126 (1983); (f) E. Yeager, *Electrochim. Acta* **29**, 1527 (1984); (g) E. Yeager, *J. Mol. Catal.* **38**, 5 (1986).
2. (a) T. Kuwana, M. Fujihira, K. Sunakawa and T. Osa, *J. Electroanal. Chem.* **88**, 299 (1978); (b) A. Bettelheim and T. Kuwana, *Anal. Chem.* **51**, 2257 (1979); (c) N. Kobayashi, M. Fujihira, K. Sunakawa and T. Osa, *J. Electroanal. Chem.* **101**, 269 (1979); (d) N. Kobayashi, M. Fujihira, T. Osa and T. Kuwana, *Bull. Chem. Soc. Jpn* **53**, 2195 (1980); (e) A. Bettelheim, R. J. H. Chan and T. Kuwana, *J. Electroanal. Chem.* **110**, 93 (1980); (f) P. A. Forshey, T. Kuwana, N. Kobayashi and T. Osa, *ACS Adv. Chem. Ser.* **201**, 601 (1982); (g) P. A. Forshey and T. Kuwana, *Inorg. Chem.* **22**, 699 (1983); (h) Y. O. Su, T. Kuwana and S.-M. Chen, *J. Electroanal. Chem.* **288**, 177 (1990).
3. A. J. Bard and L. R. Faulkner, *Electrochemical Methods, Fundamentals and Applications*, Wiley, New York, 1980, p. 675.
4. D. M. Dimarco, P. A. Forshey and T. Kuwana, *ACS Adv. Chem. Ser.* **192**, 72 (1983).
5. P. A. Forshey and T. Kuwana, *Inorg. Chem.* **20**, 693 (1981).
6. (a) N. Kobayashi, M. Koshiyama, T. Osa and T. Kuwana, *Inorg. Chem.* **22**, 3608 (1983); (b) N. Kobayashi, *Inorg. Chem.* **24**, 3324 (1985).
7. (a) R. F. Pasternack, M., A. Cobb and N. Satin, *Inorg. Chem.* **14**, 866 (1975); (b) R. F. Pasternack and M. Satin, *ibid.* **13**, 1956 (1974); (c) R. F. Pasternack, *ibid.* **15**, 643 (1976).
8. R. J. H. Chan, Y. O. Su and T. Kuwana, *Inorg. Chem.* **24**, 3777 (1985).
9. A. Bettelheim, R. Parash and D. Ozer, *J. Electrochem. Soc.* **129**, 2247 (1982).
10. D. Ozer, R. Parash, F. Broitman, U. Mor and A.

Bettelheim, *J. Chem. Soc., Faraday Trans. 1,* **80**, 1139 (1984).
11. N. Kobayashi and T. Osa, *J. Electroanal. Chem.* **157**, 269 (1983).
12. F. Arifuku, K. Iwatani, K. Ujimoto and H. Kurihara, *Bull. Chem. Soc. Jpn* **60**, 1161 (1987).
13. N. Kobayashi, T. Matsue, M. Fujihira and T. Osa, *J. Electroanal. Chem.* **103**, 427 (1979).
14. N. Kobayashi and Y. Nishiyama, *J. Electroanal. Chem.* **181**, 107 (1984).
15. (a) A. T. Kapanchan, V. S. Pshezhetski and V. S. Kavanov, *Vysokomol. Soedin., Ser. B* **11**, 5 (1969); (b) V. S. Pshezhetski, S. G. Ikryannikov, T. A. Kuzunetsova and V. A. Kavanov, *J. Polym. Sci., Polym. Chem. Ed.* **14**, 2595 (1976).
16. H. Behret, W. Clauberg and G. Sandstede, *Ber. Bunsenges. Phys. Chem.* **83**, 139 (1979).
17. N. Kobayashi and Y. Nishiyama, *J. Phys. Chem.* **89**, 1167 (1985).
18. V. G. Levich, *Physicochemical Hydrodynamics*, Prentice Hall, Englewood Cliffs, NJ, 1962.
19. N. Kobayashi, H. Shirai and N. Hojo, *J. Polym. Sci., Polym. Lett. Ed.* **27**, 191 (1989).
20. N. Kobayashi, H. Shirai and N. Hojo, *J. Chem. Soc., Dalton Trans.* 2107 (1984).
21. (a) A. M. Schaffer, M. Gouterman and E. R. Davidson, *Theor. Chim. Acta* **30**, 9 (1973); (b) H. Kobayashi and Y. Yanagawa, *Bull. Chem. Soc. Jpn* **45**, 450 (1972).
22. N. Kobayashi and A. B. P. Lever, *J. Am. Chem. Soc.* **109**, 7433 (1987).
23. (a) M. J. Stillman and A. J. Thompson, *J. Chem. Soc., Faraday Trans. 2* **70**, 790 (1974); (b) P. Day, H. A. O. Hill and M. J. Price, *J. Chem. Soc. A*, 90 (1968); (c) L. D. Rollman and R. T. Iwamoto, *J. Am. Chem. Soc.* **90**, 1455 (1968).
24. N. Kobayashi, F. Ojima, T. Osa, S. Vigh and C. C. Leznoff, *Bull. Chem. Soc. Jpn* **62**, 3469 (1989).
25. N. Kobayashi, H. Sasaki and T. Osa, *Chem. Lett.* 1917 (1985).